Design of a Dielectric-loaded Wide Beam Quad-ridged Horn Antenna

Yaqing Yu [1], Wen Jiang [1], Lv Qin [2], and Shuxi Gong [1]

[1] National Key Laboratory of Antennas and Microwave Technology
Xidian University, Xi'an, 710071, China
yuyaqing27@163.com, jw13@vip.qq.com, shxgong@xidian.edu.cn

[2] The 39th Research Institute of China Electronics Technology Group Corporation
Xi'an, 710071, China
1759803286@qq.com

Abstract ─ A quad-ridged horn antenna with dielectric loading covering the 0.6 GHz to 4 GHz band is proposed. Through the comprehensive design of differential feeding, a quad-ridged flare and loaded dielectrics, the feed antenna can be used to match a reflector with a large illumination angle of approximately 150 degrees. In the working band, the reflection coefficient is less than -8 dB, the isolation is larger than 40 dB, and its cross-polarization discrimination is larger than 31 dB for both polarizations. To verify the simulations, a prototype is fabricated and measured, and the measurements are in good agreement with the simulations. A reflector with a diameter of 33 meters and a focal diameter ratio of 0.33 is adopted to analyze the in-dish performance of the feed. The simulated results show that an average efficiency of 55.16% is realized and that the problem of the efficiency decrease caused by beamwidth narrowing at high frequencies is solved.

Index Terms ─ Dielectric loading, differential feed, quad-ridged horn, reflector antenna.

I. INTRODUCTION

Radio astronomy uses radio telescopes to study the phenomena of the universe. The performance of the antenna, the signal-receiving component of a radio telescope system, will dramatically influence the performance of the whole system.

Antennas on radio telescopes can be generally divided into two kinds: the single reflector antenna and the synthetic aperture antenna. The former is usually a large aperture reflector antenna, which mainly relies on structural technology and has the advantage of an easy replacement of the feed. The latter uses a reflector antenna or an array antenna as a unit to form the synthetic aperture radio telescope, which mainly relies on the numerical processing of a large amount of observation data. For example, the Effelsberg 100-m radio telescope, the Five-hundred-meter Aperture Spherical Telescope (FAST), the Shang Hai Astronomy Observatory (SHAO) 65-m radio telescope and the Parkes 64-m radio telescope all adopt the single reflector antenna system. Meanwhile, the Very Large Array (VLA), the Australia Telescope Compact Array (ATCA) and the Australian Square Kilometer Array Pathfinder (ASKAP) employ the synthetic aperture system. However, they are usually unable to meet the hardware requirements for a synthetic aperture radio telescope at this stage. For instance, the computation ability required by SKA is expected to be satisfied in one or two decades. Therefore, radio telescopes currently rely mainly on the single reflector antennas for observation.

For the best feed of the reflector antenna, the characteristics across the working band should be as follows: 1) dual-polarized operation, 2) good match, 3) high isolation, 4) low cross-polarization level, and 5) a nearly constant beamwidth.

Specifically, there are several kinds of feed for radio telescopes, such as a horn antenna, a phased array antenna, a log-periodic antenna and an eleven feed. In these feeds, the phased array has a flexible beam scanning capability, but its structure and feeding network are often complex, and the working bandwidth is usually not wide enough to cover a several octave band, such as the phased array feed used in the ASKAP [1, 2] and FAST [3, 4]. The log-periodic antenna used in ATA [5] and its deformation-eleven feed [6, 7] all have the problems of being difficult to match at low frequencies, to refrigerate and lacking structural robustness. Horn antennas are widely used as feeds for radio telescopes with the merits of a stable structure and easy regulation of electrical performance, such as the feed for the Goddard Geophysical and Astronomical Observatory (GGAO) 12-m radio telescope in the US, [8], the Parkes 64-m radio telescope in Australia [9] and the Effelsberg 100-m radio telescope in Germany [10, 11].

The 110-m Qi Tai Telescope (QTT), which is under construction in northwest China. It covers the 150 MHz

to 110 GHz observation band, and will soon become the largest fully steerable radio telescope in the world. The most difficult design of its feed group is the one covering the 0.6-4 GHz band, and needs to illuminates the main reflector with a diameter of 110 meters and a focal diameter ratio of 0.33 to receive the pulsar signal [8]. Combined with the previous discussion, the horn antenna is chosen as the feed for this band.

Typically, the horn antenna can be divided into the single-mode smooth-walled horn, the hybrid mode horn, the ridged horn or the lens horn. The single-mode smooth-walled horn has the simplest and most reliable structure [12]. However, due to the single-mode limitation, it has a relatively narrow working bandwidth of approximately 20% with inconsistent E and H planes in the radiation pattern. To solve the latter problem, the hybrid-mode horn antenna is presented, which can excite a certain proportion of the TM_{11} mode for a conical horn or the TE_{12}/TM_{12} mode for a pyramid horn to compensate for the asymmetry of the dominant mode on the pattern. The hybrid horn can be divided into smooth-walled multisection [13], corrugated [14], dielectric-loaded [15] and metasurface-loaded [16] types. However, the hybrid-mode technology can only broaden the working bandwidth to approximately 2.2 octaves, which is far from the required 6.7 octaves. In addition, the inconsistent beamwidths of the horn antenna in the high and the low frequencies are not instrumental in the high efficiency illumination of the reflector. A lens horn antenn modifies the field distribution on the antenna aperture by loading the dielectric [17] or metasurface [18] to enhance the gain of the main radiation direction. Although the lens loading technology does not help broaden the working bandwidth of the horn antenna, it is a good solution for solving the beamwidth inconsistency problem for high and low frequencies.

Through the capacitive loading of the ridge, the cutoff frequency of the dominant mode for a ridged horn is lowered, and then the working band is expanded. To meet the requirements of a dual-polarized operation, a quad-ridged horn antenna should be adopted. However, the traditional quad-ridged horn antenna suffers from the efficiency decreasing at high frequencies due to the inherent narrowing of the beamwidths [8]. To solve this problem, dielectric loading technology is applied to the design of a quad-ridged horn antenna. However, the gain can only be enhanced across the whole band when a ball-like [19] or cone-like [20] lens is loaded onto the aperture, without narrowing the beamwidth difference between high and low frequencies. By loading a three-layered spear-like dielectric, a nearly constant-beam feed with a 12 dB beamwidth of approximately 100 degrees in 6 octaves is realized [9]. Since the illumination angle of the QTT's main reflector needs to reach approximately 150 degrees, obviously, none of the above feeds meet the requirement. A single-layered cylindrical dielectric is

loaded to achieve a 150-degree illumination of a 100-m reflector [21]. However, the feed is failed to generate sufficient hybrid-mode of HE_{11} to reduce the beamwidth difference between E and H planes of the radiation patterns.

In this paper, a quad-ridged horn antenna based on dielectric loading is proposed, covering the 0.6 GHz to 4GHz band. By applying differential feeding, the special ridge and dielectric loading technology, the feed can realize the characteristics of a nearly constant beamwidth, a low cross-polarization level and a high isolation in nearly 7 octaves. To match the QTT's 110-m reflector, the horn antenna's 12 dB beamwidth reaches nearly 150 degrees in most in-band frequencies. The corresponding phase of the electric field in the angular domain is maintained within ±20 degrees. To verify the design, a prototype is fabricated and measured, and the results are compared with the simulations.

The remainder of the paper is arranged as follows. Section II mainly describes the structure and design procedure of the antenna. In Section III, a prototype is fabricated and measured to verify the proposed design. The in-dish performance of the antenna combined with the reflector is determined in Section IV. Finally, a brief summary is given in Section V.

II. ANTENNA DESIGN

This section mainly describes the structure introduction, the beam control mechanism and the design process of the proposed antenna.

A. Structure introduction

The horn antenna, including the differential feeding structure, the loaded dielectrics and the quad-ridged flare part, is shown in Fig. 1 and is explained below.

The differential feeding structure consists of four differential feeding coaxial cables and the coaxial cable to the quad-ridged waveguide transition, which can suppress the higher order modes, especially the pattern deterioration mode of TE_{21L} [22]. In addition, compared with the traditional criss-crossed side feeding structure, the bottom differential feeding technology provides a fully asymmetry, which brings the working characteristics of the antenna's two polarizations closer.
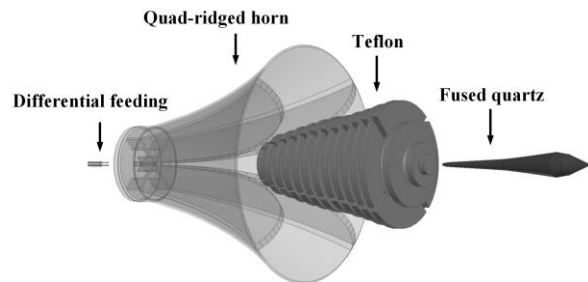
Fig. 1. The structural sketch of the horn antenna.
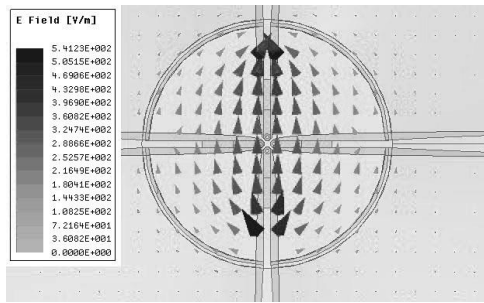
Fig. 2. The sectional electric field distribution of the horn antenna excited by differential feeding.

As for the cross-polarization, due to the fully axisymmetric structure, the electric field vectors orthogonal components excited on each side of the stimulated double ridge pair are equal in magnitude but opposite in phase, shown in Fig. 2. When the out-of-phase components of the two groups are closer in magnitude, the superposition and cancellation of the components formed in the far-field will be more thorough [23]. As a result, the symmetry of the structure can ensure the high cross polarization discrimination of the feed at the same time.

The dielectric part is composed of Teflon and fused quartz. The fused quartz has a spear-like shape with a dielectric constant of 3.82, which is outlined by multiple lines. The Teflon has a dielectric constant of 2.1 and consists of two parts: the inner part is solid except the hollow space reserved for the fused quartz; the outer part is cut with grooves to realize a lower equivalent permittivity. To mount on the quad-ridged horn, the parts of the Teflon is cut out the space for the four ridges. These dielectrics are set along the central axis of the quad-ridged horn, whose bottoms are located at the beginning of the taper section of the horn.

The outline of the special ridge of the quad-ridged horn is formed by several straight lines, two exponential lines and one arc. The detailed design of these parts will be discussed in part C.

B. Beam control mechanism

If the reflector feed has a constant beamwidth characteristic within the working bandwidth, it will help to improve the efficiency of the reflector antenna. To achieve the characteristics above, we can adopt the following ideas for a dielectric-loaded quad-ridged horn antenna.

As for medium and low frequencies, the radiation pattern is mainly determined by the structural parameters. Of all the parameters describing the quad-ridge horn geometry, the ridges and sidewall play the most critical roles in determining the performance of the horn [8].

For high frequencies, the field distribution is mainly concentrated between the two corresponding ridges when a polarization is stimulated. Considering that the

dielectric rod antenna can control the radiation pattern by adjusting the dielectric shape [24], the dielectric rod can also be used to broaden the high frequencies' beamwidth when the dielectric constant of each layer changes in the gradient form. The composite antenna working in high frequencies can be seen as a dielectric rod antenna excited by the quad-ridged waveguide. At the same time, it has the quad-ridged flare around the rod to regulate and suppress the fields of some high-order modes. From another perspective, it can also be understood as a quad-ridged horn antenna that regulates the aperture field distribution by dielectric loading. As a result, the narrowing problem of the radiation pattern at high frequencies can be effectively solved by dielectric loading.

The beamwidth characteristic of the feed should match the f/D ratio of the reflector. For traditional conical or pyramidal feed horns, the commonly adopted illumination level of the feed is -10 dBi. However, for modern high-efficiency hybrid-mode feed horns, the feed factor of G/T will reach a maximum when illumination level of the feed is approximately -16 dB [25]. Since the distance between the feed and each point of the reflector is not the same, there exists spatial diffusion attenuation between the center and the edge of the reflector. Therefore, to form the best illumination, the spatial diffusion attenuation needs to be considered. For instance, for a reflector with an f/D ratio of 0.33, the best illumination angle is approximately ±74 degrees, and the spatial diffusion attenuation at the edge is approximately 3.8 dB [26]. As a result, the illumination level of the designed feed should be -12.2 dBi. Two illumination cases for the traditional and designed feeds are shown in Fig. 3.

C. Design process

First, we aim to design a quad-ridged horn antenna without dielectric loading. We divide the design into two parts: the transition from coaxial cables to a quad-ridged waveguide and the quad-ridged horn.

(a)   (b)
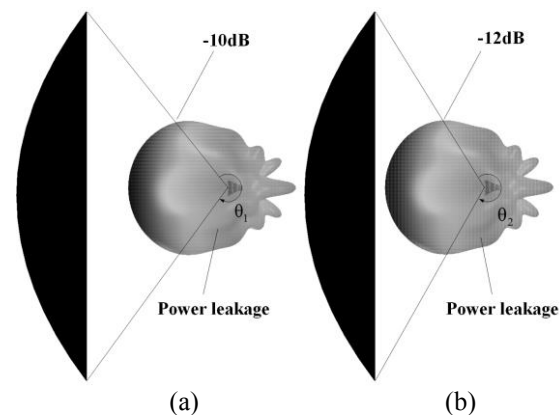
Fig. 3. The schematic diagrams of illumination level comparison for the feed: (a) the case for traditional feed, and (b) the case for designed feed.

The antenna is differentially fed by four coaxial connectors in the bottom, with each pair stimulating a polarization. Since the start frequency of our design is 0.6 GHz, the cutoff frequency of the quad-ridged waveguide should be 0.48 GHz to guarantee an allowance of 25%. According to the normalized cutoff wavenumbers of the circular quad-ridged waveguide [27], the ratio of the ridge spacing to the circular waveguide diameter should be as small as possible to obtain the widest bandwidth. When the ratio is close to 0, the cutoff frequency can be reduced to approximately one half of the circular hollow waveguide. Therefore, the diameter of the quad-ridged waveguide should be designed as the cutoff wavelength of the circular hollow waveguide at 0.96 GHz. The simplified equation for the cutoff frequency of the TE_{11} mode in a hollow circular waveguide can be expressed as follows [28],

$$f_c = \frac{c}{4\pi} \frac{p'_{11}}{a},$$ (1)

where c is the speed of light in free space, a is the diameter of the circular waveguide and p'_{11} is the first zero of the derivative of the first-order Bessel function.

From (1), we can get that the cutoff wavelength of the TE_{11} mode at 0.96 GHz is approximately 183.2 mm. Therefore, the theoretical diameter of the quad-ridged waveguide should be larger than 91.6 mm. All four ridges are chamfered to achieve a smaller ridge spacing. A concave structure at the bottom of the ridge is adopted to adjust the broadband matching characteristics from the coaxial cable to the quad-ridged waveguide [9].

The detailed structural parameters of the transition are shown in Fig. 4. With the help of the full-wave simulation software ANSYS HFSS 15, the transition is optimized to work in the 0.6 GHz to 4 GHz band, as shown in Fig. 5.

The far-field characteristics are mainly determined by the quad-ridged horn. For the target performance of a 12 dB beamwidth of 150 degrees, the maximum gain of the antenna at medium frequencies should be controlled to approximately 9 dBi. As mentioned in part B, we analyze different ridges and sidewalls, with the diagram of controlling parameters of the four ridges depicted in Fig. 6. The inner special ridge curve is composed of an exponential line and a tangent arc, where the exponential part can be expressed as follows:

$$y_{inner} = \frac{d}{2} e^{\ln(\frac{a_2 - 2b_1h_2}{d}) \cdot \frac{z}{h_2}} + b_1 z,$$ (2)

where d is the spacing of the ridged waveguide, a_2 is the aperture diameter of the horn, h_2 is the height controlling parameter of the exponential curve, and b_1 is the linear part controlling parameter of the exponential curve.

(a)　　　　　　(b)
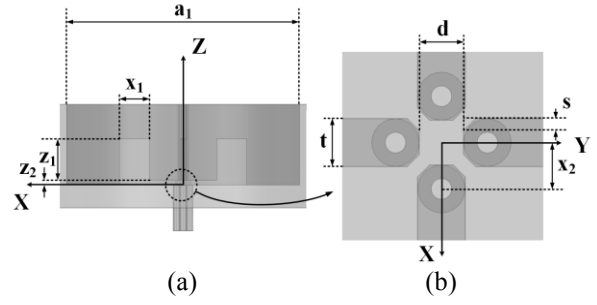
Fig. 4. Structural parameters of the transition. The optimized parameters are (unit: mm): a_1=52.5, x_1=13.1, x_2=1.5, z_1=17.9, z_2=2.1, d=2.8, t=3, s=0.75: (a) side view, and (b) top view of the dotted part.
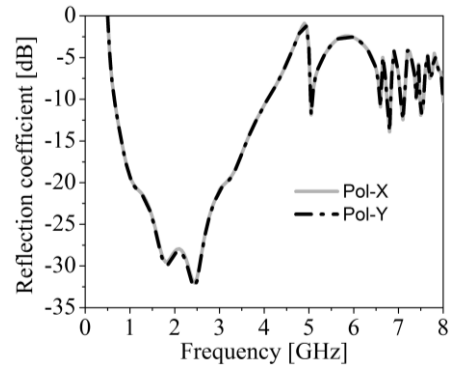
Fig. 5. The reflection coefficients for two polarizations of the transition.
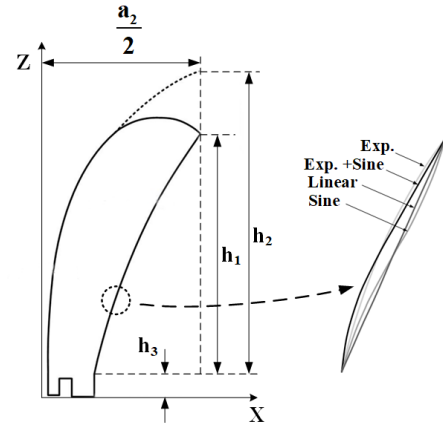
Fig. 6. Profile sketch of the ridge and the side wall.

The curve of side wall can be expressed as follows:

$$y_{outer} = \frac{a_1}{2} e^{\ln(\frac{a_2 - 2b_2h_1}{a_1}) \cdot \frac{z}{h_1}} + b_2 z,$$ (3)

where a is the diameter of the quad-ridged waveguide, h_1 is the height controlling parameter of the exponential curve, and b_2 is the linear part controlling parameter of the exponential curve.

Different from a traditional exponential ridge, the special ridge has a more compact size and a lighter weight. This structure can also improve the high frequency pattern deterioration problem to some extent [29].

By controlling the parametrics b_1 and h_2, we can adjust the distance variation speed of each pair of ridges when d and a_2 are fixed. As is known, the ridge and sidewall mainly affect the beamwidth in the middle-frequency band (1 GHz to 1.7 GHz), while the beamwidth in the high-frequency band (1.7 GHz to 4 GHz) can be controlled by the dielectrics mentioned below [9]. Therefore, we aim to determine a set of parameters that can guarantee a good in-band reflection and make the antenna's gain close to 9 dBi in the middle-frequency band. Since the ridge curve has been discussed in reference [8], here, we compare the linear, exponential, sinusoids and exponential combined sinusoids types. Some contrast simulations are given in Fig. 7, such as comparisons of different b_1, h_2 and sidewall types.

(g)
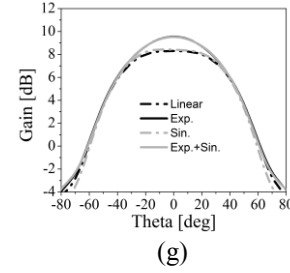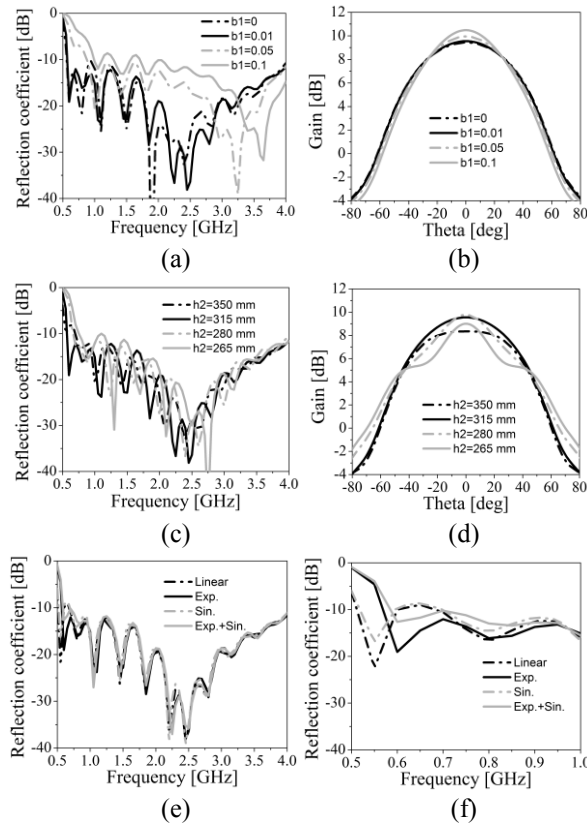
Fig. 7. Contrast simulations of the ridges and sidewall: (a) reflection coefficient with different b_1,.(b) radiation pattern at 1.5GHz with different b_1 when X-pol. is stimulated, (c) reflection coefficient with different h_2, (d) radiation pattern at 1.5 GHz with different h_2 when X-pol. is stimulated, (e) reflection coefficient with different side wall type, (f) detailed reflection coefficient with different sidewall types, and (g) radiation pattern at 1.5 GHz with different sidewall type when X-pol. is stimulated.

From Fig. 7 we can see that by selecting reasonable parameters, the performance of the reflection and far-field characteristics can satisfy the requirements.

As a result, $b_1=0.01$, $h_2=335mm$ and an exponential curve with a linear part of $b_2=0.01$ for the sidewall are chosen to achieve good in-band matching and close to 9 dBi gain characteristics.

The quad-ridged horn is depicted in Fig. 8, and its electrical characteristics are shown in Fig. 9. The antenna working from 0.6 GHz to 4 GHz has a good reflection performance less than -10 dB, a polarization isolation larger than 60 dB and a cross-polarization level less than -40 dB. However, from Figs. 9. (e) and (f) we can determine that the beamwidths at low and high frequencies are quite different, and the latter are too narrow, which do not match with the main reflector of the QTT.

(a)

(b)

(c)

(d)

(e)

(f)

Fig. 8. Modelling of the quad-ridged horn.

(a)   (b)

(c)   (d)

(e)   (f)
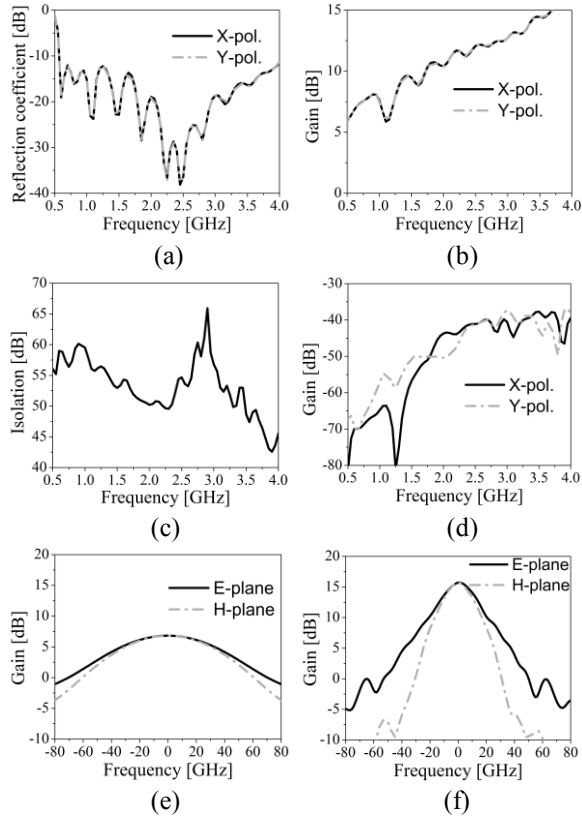
Fig. 9. Simulation of the quad-ridged horn: (a) reflection coefficient, (b) gain in the Z-axis direction, (c) isolation of two polarizations, (d) cross-polarization level in the Z-axis direction, (e) radiation pattern at 0.6GHz when X-pol. is stimulated, and (f) radiation pattern at 4GHz when X-pol. is stimulated.

As mentioned in part B, here, we conduct some work about the dielectric loading. First, we study the case of single-layered dielectric loading, as depicted in Fig. 10. The dielectric adopts a fused quartz with a dielectric constant of 3.82, which is composed of two cones.

Through the parameter study of the single-layered dielectric, we can see that the shape change of the dielectric can affect the radiation characteristics, as shown in Fig. 11. However, the load of single-layered dielectric is not sufficient to cover all the high frequencies.

Then, the second layer of dielectric is added, which applies the PTFE with a dielectric constant of 2.1, as depicted in Fig. 12. Similar to the above, we study the shape parameters of the second layer when the parameters of the inner dielectric are set as: D_1=36 mm, h_4=200 mm and h_5=60 mm. From the comparison results in Fig. 13, we pick out a group of parameters that has a relative stable gain across the band. The specific parameters are as follows: D_2=30 mm, D_3=130 mm, h_6=220 mm and h_7=52 mm.

(a)   (b)

(c)
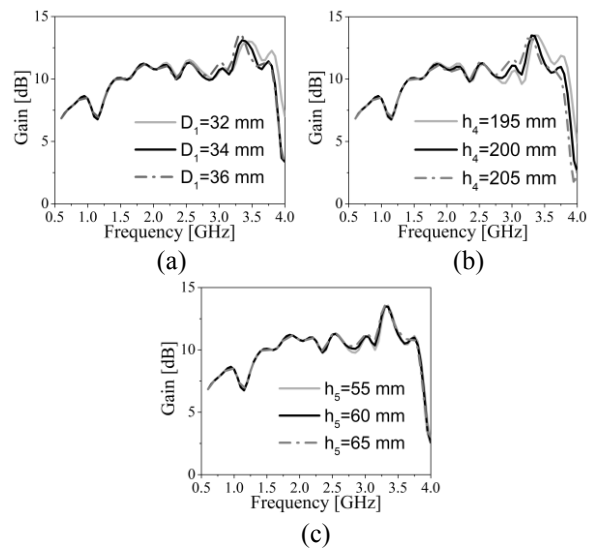
Fig. 11. Gain variation curves in main radiation direction: (a) study of D_1 when h_4=200 mm and h_5=60 mm are fixed, (b) study of h_4 when D_1=36 mm and h_5=60 mm are fixed, and (c) study of h_5 when D_1=36 mm and h_4=200 mm are fixed.

Fig. 10. The sectional view of the single-layered case.
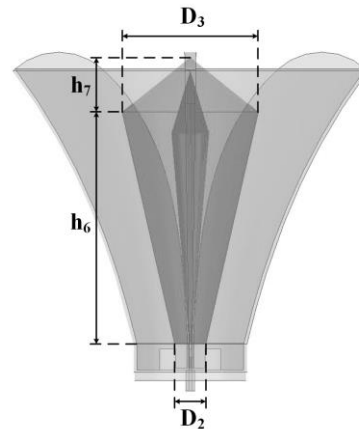
Fig. 12. The sectional view of the double-layered case.
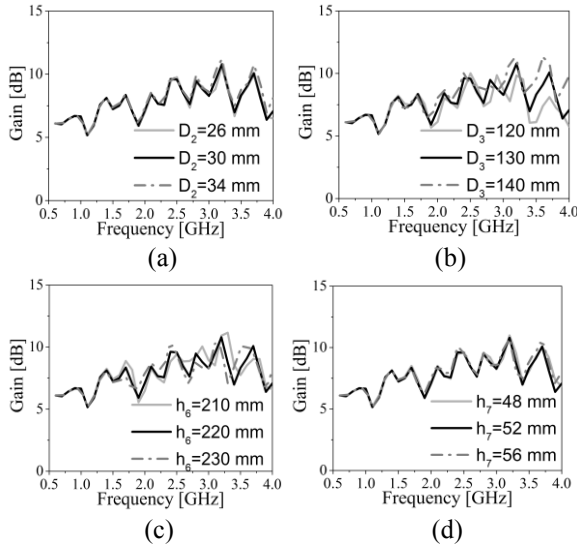
Fig. 13. Gain variation curves in main radiation direction: (a) D_3=130 mm, h_6=220 mm and h_7=52 mm are fixed, (b) D_2=30 mm, h_6=220 mm and h_7=52 mm are fixed, (c) D_2=30 mm, D_3=130 mm and h_7=52 mm are fixed, and (d) D_2=30 mm, D_3=130 mm and h_6=220 mm are fixed.

However, in the form of double-layered dielectric loading, the gain in the main radiation direction cannot be adjusted to 9 dBi for most high frequencies. Therefore, based on this double-layered design, the third layer is added to optimize the radiation characteristics. To achieve a lower equivalent dielectric constant, the dielectric of the PTFE cut with grooves is adopted. With the help of ANSYS HFSS 15, the final dielectric design is optimized, as shown in Fig. 14. The performance of the dielectric-loaded horn antenna will be presented in the next section.
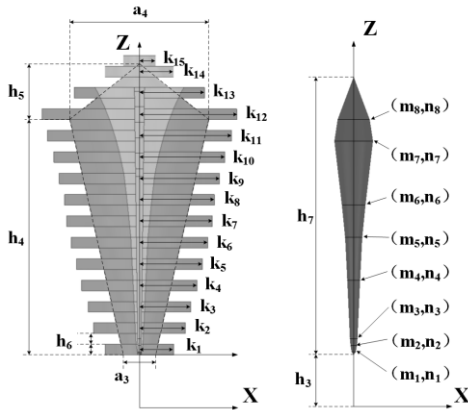
Fig. 14. The sectional view of the optimized dielectrics. The optimized parameters are (unit: mm): h_3=25, h_4=220, h_5=52, h_6=10, h_7=260, a_3=30, a_4=130, k_1=32, k_2=43, k_3=48, k_4=54, k_5=59, k_6=64, k_7=68, k_8=70, k_9=75, k_{10}=80, k_{11}=86, k_{12}=91, k_{13}=61, k_{14}=32, k_{15}=15, m_1=2, n_1=28, m_2=3, n_2=34, m_3=3.5, n_3=40, m_4=6, n_4=95, m_5=8, n_5=135, m_6=11, n_6=165, m_7=18, n_7=225, m_8=15, n_8=245.

To further analyze the effect of dielectric loading, the electric field distributions in the diagonal plane of the antenna before and after loading the dielectrics are given in Fig. 15. It can be seen from the comparison that the electric field distributions of the latter are more identical. To confirm this, the antenna aperture electric field distributions of the latter are depicted in Fig. 16.
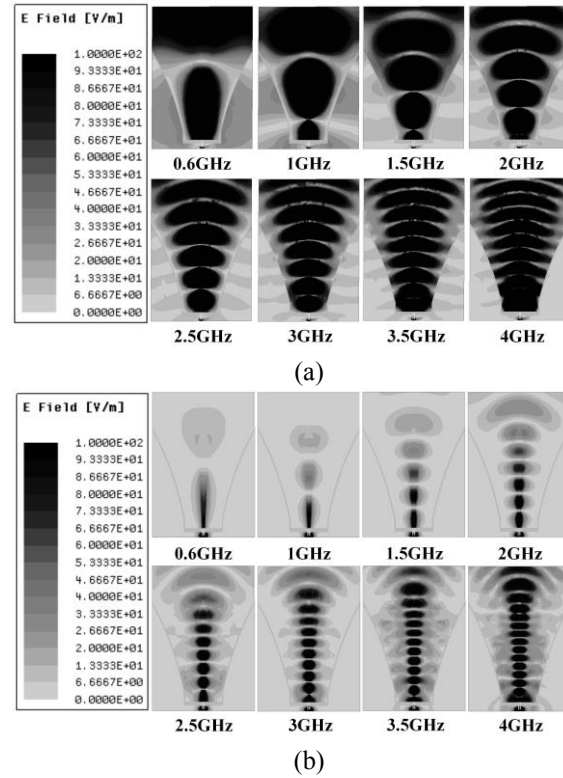
Fig. 15. Electric field distributions of the antenna in the diagonal plane: (a) quad-ridged horn without dielectric loading, and (b) quad-ridged horn with dielectric loading.
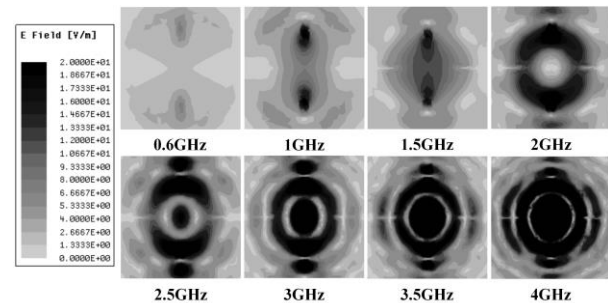
Fig. 16. Aperture electric field distributions of the antenna.

To verify the simulation, a prototype is fabricated. The reflection coefficient and the radiation pattern characteristics are measured and compared with the simulation.

III. MODELING AND EXPERIMENTAL RESULTS

The electrical characteristics of the proposed dielectric-loaded quad-ridged horn antenna are analyzed by using ANSYS HFSS 15. A prototype of the feed antenna is manufactured and tested, as shown in Fig. 17. The metal parts including the ridges, the flared horn and the back cavity are fabricated with CNC milling technology. For the dielectrics, the cylinders are first made by casting molding technology, and then CNC milling technology is utilized to obtain the designed shape. To facilitate the test, we use a transmission line balun to differentially feed the antenna.

The simulated and measured results are demonstrated in Fig. 18. The proposed antenna possesses a reflection coefficient of less than -8 dB across the working band of 0.6 GHz to 4 GHz, and less than -10 dB for most frequencies, as shown in Fig. 18 (a). The isolation is larger than 40 dB, and its cross-polarization discrimination is larger than 31 dB for both polarizations, as shown in Fig. 18 (b) and Fig. 18 (c). From (c), we can also see that the gains in medium and high frequency ranges are highly suppressed to approximately 9 dBi. Due to the symmetry structure and differential feeding technology, the isolation and cross-polarization level are both very low.

From (d), the 12 dB beamwidth of E and H plane are close to each other at most frequencies, with an average difference of 33 degrees. To verify the simulated beamwidths of the feed, figure (f) to (h) give the radiation pattern comparisons of 0.6 GHz, 2.5 GHz and 4 GHz. From the results, we can see that the simulations are in good agreement with the measurements.

Fig. 17 The antenna under testing in a microwave anechoic chamber.

As seen with the beamwidth, the phase consistency of the wavefront is a very important parameter for the reflector feed. The simulated equal phase angle (defined as the angular range of the phase fluctuation being less than ±20 degrees) of the radiated electric field is depicted in Fig. 18 (e), when the observation point is located on the Z axis and 250 mm above the antenna bottom. The simulated distance from the antenna bottom to the phase center is also depicted in (e), which shows it to be stable to 240±20 mm across the 1.7-4.2 GHz band.

The differences between the simulations and measurements are mainly caused by the reflection and phase imbalance brought from the balun, machine errors and test errors. For example, we find that when the balun is connected with a long transmission line, some resonances will be produced, which will affect the reflection and phase characteristics.

To further verify the performance of the feed in the reflector system, the in-dish simulation of the reflector antenna is carried out in the next section.

(a)

(b)

(c)

(d)

(g)

(e)

(h)

(f)
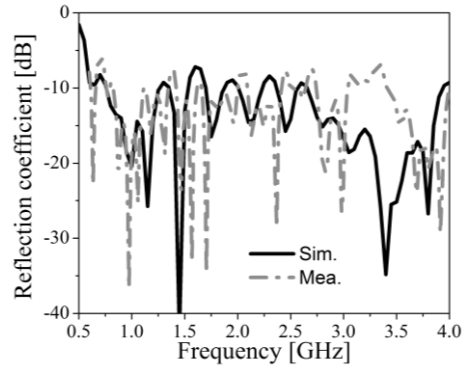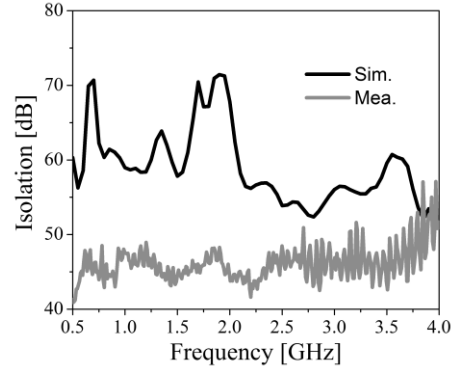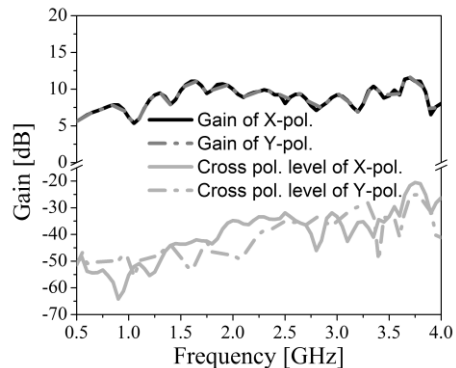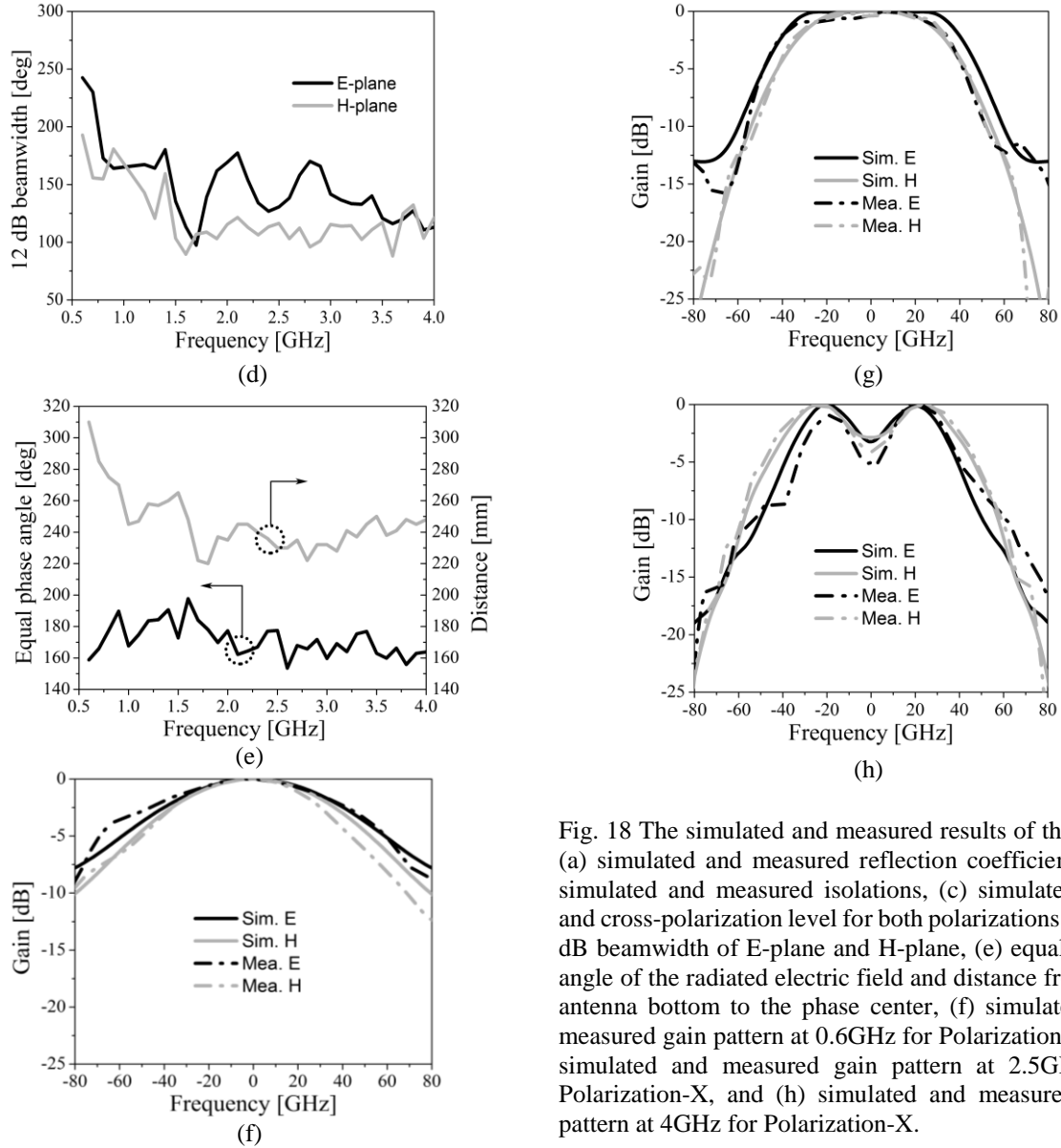
Fig. 18 The simulated and measured results of the feed: (a) simulated and measured reflection coefficients, (b) simulated and measured isolations, (c) simulated gain and cross-polarization level for both polarizations, (d) 12 dB beamwidth of E-plane and H-plane, (e) equal phase angle of the radiated electric field and distance from the antenna bottom to the phase center, (f) simulated and measured gain pattern at 0.6GHz for Polarization-X, (g) simulated and measured gain pattern at 2.5GHz for Polarization-X, and (h) simulated and measured gain pattern at 4GHz for Polarization-X.

Table 1: The comparison between other dielectric loaded quad-ridged horn antennas

Ref.	Reflection/ dB	Band/ GHz	Isolation/ dB	XPD/ dB	f/D of Matched Reflector	Avg. Aperture Efficiency	Avg. Diff. between E and H Plane/deg
[9]	<-15	0.7-4.2	>45	>28	0.41	65%	N/A
[19]	<-7	5-15	>45	>28	N/A	N/A	N/A
[21]	<-7	1.5-15.5	>40	>15	0.3	50%	~51
This work	<-8	0.6-4	>40	>31	0.33	55%	33

XPD: cross-polarization discrimination; f/D: focal diameter ratio; Avg.: average; Diff.: difference

IV. IN-DISH SIMULATION WITH REFLECTOR

The feedforward mode is adopted for the feed to illuminate the main reflector of the QTT in the 0.6 GHz to 4 GHz band. With the help of the HFSS-IE function, we can analyze the in-dish performance of the feed. However, due to the limitation of computational resource, here we can only calculate the performance of the feed on a scaled 33-m parabolic reflector with the same focal diameter ratio of 0.33. In this simulation, the

phase center of the feed, which is 250 mm above the antenna bottom, is put at the focus of the 33-m reflector. The main radiation direction of the antenna is aligned with the center point of the reflector, as illustrated in Fig. 19. Then, we can determine the efficiency of the reflector antenna by processing the theoretical gain and simulated gain. The aperture efficiency of the reflector antenna is shown in Fig. 20, and the theoretical gain can be expressed as the following formula:

$$Gain = 10\log(\frac{4\pi A\eta}{\lambda^2}),$$

where A represents the aperture area of the antenna, λ denotes the working wavelength, η represents the efficiency and $\eta=1$ when calculating the theoretical gain.

From the results, we can see that the efficiency of the antenna can be maintained at 46%-67% in the working frequency band. An average efficiency of 55.16% can make the reflector antenna work normally.
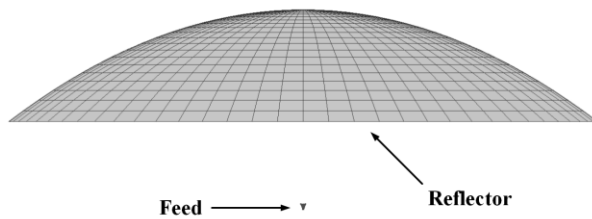
Fig. 19 Diagram of the reflector antenna.
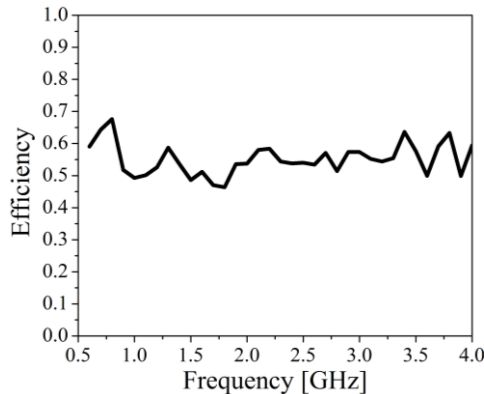
Fig. 20 The efficiency of the reflector antenna.

V. CONCLUSION

A dielectric-loaded quad-ridged horn antenna was proposed for operation in the 0.6 GHz to 4 GHz. The design procedure of the quad-ridged horn antenna and loaded dielectrics were presented to realize a nearly constant beamwidth characteristic in middle and high frequencies. Then, to verify the performance, the feed was fabricated and measured. The simulations and measurements were in good agreement. In the end, the in-dish simulation of the feed was performed to verify the efficiency of reflector antenna. The results showed

that the antenna can be a feed candidate of the QTT's main reflector for the pulsar observation band.

REFERENCES

[1] D. R. DeBoer, *et al.*, "Australian SKA pathfinder: A high-dynamic range wide-field of view survey telescope," *Proceedings of the IEEE*, vol. 97, no. 8, pp. 1507-1521, July 2009.

[2] A. Chippendale, *et al.*, "Phased array feed testing for astronomy with ASKAP," *2010 IEEE International Symposium on Phased Array Systems and Technology*, Waltham, MA, USA, pp. 648-652, Oct. 2010.

[3] D. Li and Z. C. Pan, "The five-hundred-meter aperture spherical radio telescope project," *Radio Science*, vol. 51, no. 7, pp. 1060-1064, Dec. 2016.

[4] Y. Wu, K. F. Warnick, and C. J. Jin, "Design study of an L-band phased array feed for wide-field surveys and vibration compensation on FAST," *IEEE Transactions on Antennas and Propagation*, vol. 61, no. 6, pp. 3026-3033, Mar. 2013.

[5] D. R. DeBoer and D. C. J. Bock, "The Allen telescope array: Splitting the aperture," *IEEE Microwave Magazine*, vol. 5, no. 2, pp. 46-53, June 2004.

[6] J. Yang, *et al.*, "Cryogenic 2–13 GHz eleven feed for reflector antennas in future wideband radio telescopes," *IEEE Transactions on Antennas and Propagation*, vol. 59, no. 6, pp. 1918-1934, Mar. 2011.

[7] J. Yang, *et al.*, "A compact dual-polarized 4-port eleven feed with high sensitivity for reflectors over 0.35–1.05 GHz," *IEEE Transactions on Antennas and Propagation*, vol. 63, no. 12, pp. 5955-5960, Oct. 2015.

[8] A. Akgiray, *et al.*, "Circular quadruple-ridged flared horn achieving near-constant beamwidth over multioctave bandwidth design and measurements," *IEEE Transactions on Antennas and Propagation*, vol. 61, no. 3, pp. 1099-1108, Mar. 2013.

[9] A. Dunning, *et al.*, "An ultra-wideband dielectrically loaded quad-ridged feed horn for radio astronomy," *2015 IEEE-APS Topical Conference on Antennas and Propagation in Wireless Communications (APWC)*, Turin, Italy, pp. 787-790, Oct. 2015.

[10] W. HeB and B. Liesenkotter, "A dual mode horn feed for deep space telemetry reception by the Effelsberg radio telescope," *1973 3rd European Microwave Conference*, Brussels, Belgium, Sept. 1973.

[11] J. Flygare, M. Pantaleev, and S. Olvhammar, "BRAND: Ultra-wideband feed development for

the European VLBI network — A dielectrically loaded decade bandwidth quad-ridge flared horn," *12th European Conference on Antennas and Propagation (EuCAP 2018)*, London, UK, Apr. 2018.

[12] K. T. Selvan, *et al.*, "Accurate design method for pyramidal horns of any desired gain and aperture phase error," *IEEE Antennas and Wireless Propagation Letters*, vol. 7, pp. 31-32, Feb. 2008.

[13] D. A. Monto, *et al.*, "High-performance smooth-walled horn antennas for THz frequency range: Design and evaluation," *IEEE Transactions on Terahertz Science and Technology*, vol. 9, no. 6, pp. 587-597, Sept. 2019.

[14] S. S. Roy, *et al.*, "Design of a compact multielement monopulse feed for ground-station satellite tracking applications," *IEEE Antennas and Wireless Propagation Letters*, vol. 18, no. 9, pp. 1721-1725, July 2019.

[15] S. Zhang, D. Cadman, and J. Y. C. Vardaxoglou, "Additively manufactured profiled conical horn antenna with dielectric loading," *IEEE Antennas and Wireless Propagation Letters*, vol. 17, no. 11, pp. 2128-2132, Sept. 2018.

[16] Q. Wu, *et al.*, "A Ku-band dual polarization hybrid-mode horn antenna enabled by printed-circuit-board metasurfaces," *IEEE Transactions on Antennas and Propagation*, vol. 61, no. 3, pp. 1089-1098, Nov. 2012.

[17] G. B. Wu, *et al.*, "High-gain circularly polarized lens antenna for terahertz applications," *IEEE Antennas and Wireless Propagation Letters*, vol. 18, no. 5, pp. 921-925, Mar. 2019.

[18] K. T. Liu, Y. H. Ge, and C. X. Lin, "A compact wideband high-gain metasurface-lens-corrected conical horn antenna," *IEEE Antennas and Wireless Propagation Letters*, vol. 18, no. 3, pp. 457-461, Jan. 2019.

[19] Y. Li, Z. Y. Zhang, and G. Fu, "A design of quad-ridged horn antenna with dielectric loading," *2014 XXXIth URSI General Assembly and Scientific Symposium (URSI GASS)*, Beijing, China, Oct. 2014.

[20] R. J. Bauerle, *et al.*, "The use of a dielectric lens to improve the efficiency of a dual-polarized quad-ridge horn from 5 to 15 GHz," *IEEE Transactions on Antennas and Propagation*, vol. 57, no. 6, pp. 1822-1825, June 2009.

[21] J. Flygare and M. Pantaleev, "Dielectrically loaded quad-ridge flared horn for beamwidth control over decade bandwidth—optimization, manufacture, and measurement," *IEEE Transactions on Antennas and Propagation*, vol. 68, no. 1, pp. 207-216, Sept. 2019.

[22] T. S. Beukman, *et al.*, "A quadraxial feed for ultra-wide bandwidth quadruple-ridged flared horn antennas," *The 8th European Conference on Antennas and Propagation (EuCAP 2014)*, The Hague, Netherland, pp. 3312-3316, Sept. 2014.

[23] Q. Xue, S. W. Liao, and J. H. Xu, "A differentially-driven dual-polarized magneto-electric dipole antenna," *IEEE Transactions on Antennas and Propagation*, vol. 61, no. 1, pp. 425-430, Jan. 2013.

[24] C. W. Liu and C. C. Chen, "A UWB three-layer dielectric rod antenna with constant gain, pattern and phase center," *IEEE Transactions on Antennas and Propagation*, vol. 60, no. 10, pp. 4500-4508, Oct. 2012.

[25] G. L. James and B. MacA. Thomas, "Comparison of G/T between dual-reflector and primary-focus antennas," *Electronics Letters*, vol. 16, no. 8, pp. 286-288, Apr. 1980.

[26] J. L. Volakis, *Antenna Engineering Handbook*, 4nd ed., McGraw-Hill, New York, 2007.

[27] W. M. Sun and C. A. Balanis, "Analysis and design of quadruple-ridged waveguides," *IEEE Transactions on Antennas and Propagation*, vol. 42, no. 12, pp. 2201-2207, Dec. 1994.

[28] N. Marcuvitz, *Waveguide Handbook*, ser. MIT Radiation Laboratory. Lexington, MA: Boston Technical, 1964.

[29] B. Jacobs, J. W. Odendaal, and J. Joubert, "An improved design for a 1–18 GHz double-ridged guide horn antenna," *IEEE Transactions on Antennas and Propagation*, vol. 60, no. 9, pp. 4110-4118, July 2012.

Yaqing Yu was born in Zhejiang Province, China, in October 1990. He received the B.S. degree in Electromagnetic Field and Wireless Technology from Xidian University, Xi'an, China, in 2009. He is currently studying for a doctor's degree in Electromagnetic Field and Microwave Technology from Xidian University. His research interests include wideband antennas, wide beam antennas and antenna feeding structures.

Wen Jiang was born in Shandong Province, China, in November 1985. He received the B.S. and Ph.D. degrees from Xidian University, Xi'an, China, in 2008 and 2012, respectively. He is the Vice Director of the National Key Laboratory of Science and Technology on

Antennas and Microwaves, Xidian University, where he is currently an Associate Professor. His current research interests include electromagnetic scattering and stealth technology, antenna theory and engineering, and electromagnetic measurement theory and technology.

Lv Qin was born in Guangxi Province, China, in 1979. He received his bachelor's degree in Computer Communications from the College of Electronic Information, Sichuan University. He is currently a Senior Engineer at the 39th Research Institute of China Electronics Technology Group Corporation. He has presided over or participated in many 863 and 973 National Key R&D projects about the design of feed systems, such as high-power measurement radar, TT&C antenna and radio telescope antenna. His current research interests include the design of horn antenna, feed antenna and core components of the feed.

Shuxi Gong was born in Hebei Province, China, in March 1957. He received the B.S. and M.S. degrees from Xidian University, Xi'an, China, in 1982 and 1984, respectively, and the Ph.D. degree from Xi'an Jiaotong University, Xi'an, in 1988. He was the Director of the National Key Laboratory of Science and Technology on Antennas and Microwaves, Xidian University, where he is currently a Full Professor. He has authored or coauthored over 200 refereed journal papers. He has also authored Principles of Generalized Eigenfunction Expansions in Electro-magnetic Theory (Xi'an: Xidian Univ. Press, 2010), Prediction and Reduction of Antenna Radar Cross Section (Xi'an: Xidian Univ. Press, 2010), and Antennas for Mobile Communication Systems (Beijing: Electronics Industry Press, 2011). His current research interests include antenna theory and technology, prediction and control of antenna radar cross section (RCS), and RCS calculation of complex targets.